JVI Journals.ASM.org

Enhancement of Blood-Brain Barrier Permeability and Reduction of Tight Junction Protein Expression Are Modulated by Chemokines/Cytokines Induced by Rabies Virus Infection

Qingqing Chai,[a,b] Wen Q. He,[b] Ming Zhou,[a,b] Huijun Lu,[b] Zhen F. Fu[a,b]

State-Key Laboratory of Agricultural Microbiology, College of Veterinary Medicine, Huazhong Agricultural University, Wuhan, China[a]; Department of Pathology, College of Veterinary Medicine, University of Georgia, Athens, Georgia, USA[b]

ABSTRACT

Infection with laboratory-attenuated rabies virus (RABV) enhances blood-brain barrier (BBB) permeability, which has been demonstrated to be an important factor for host survival, since it allows immune effectors to enter the central nervous system (CNS) and clear RABV. To probe the mechanism by which RABV infection enhances BBB permeability, the expression of tight junction (TJ) proteins in the CNS was investigated following intracranial inoculation with laboratory-attenuated or wild-type (wt) RABV. BBB permeability was significantly enhanced in mice infected with laboratory-attenuated, but not wt, RABV. The expression levels of TJ proteins (claudin-5, occludin, and zonula occludens-1) were decreased in mice infected with laboratory-attenuated, but not wt, RABV, suggesting that enhancement of BBB permeability is associated with the reduction of TJ protein expression in RABV infection. RABV neither infects the brain microvascular endothelial cells (BMECs) nor modulates the expression of TJ proteins in BMECs. However, brain extracts prepared from mice infected with laboratory-attenuated, but not wt, RABV reduced TJ protein expression in BMECs. It was found that brain extracts from mice infected with laboratory-attenuated RABV contained significantly higher levels of inflammatory chemokines/cytokines than those from mice infected with wt RABV. Pathway analysis indicates that gamma interferon (IFN-γ) is located in the center of the cytokine network in the RABV-infected mouse brain, and neutralization of IFN-γ reduced both the disruption of BBB permeability *in vivo* and the downregulation of TJ protein expression *in vitro*. These findings indicate that the enhancement of BBB permeability and the reduction of TJ protein expression are due not to RABV infection *per se* but to virus-induced inflammatory chemokines/cytokines.

IMPORTANCE

Previous studies have shown that infection with only laboratory-attenuated, not wild-type, rabies virus (RABV) enhances blood-brain barrier (BBB) permeability, allowing immune effectors to enter the central nervous system (CNS) and clear RABV from the CNS. This study investigated the mechanism by which RABV infection enhances BBB permeability. It was found that RABV infection enhances BBB permeability by downregulation of tight junction (TJ) protein expression in the brain microvasculature. It was further found that it is not RABV infection *per se* but the chemokines/cytokines induced by RABV infection that downregulate the expression of TJ proteins and enhance BBB permeability. Blocking some of these cytokines, such as IFN-γ, ameliorated both the disruption of BBB permeability and the downregulation of TJ protein expression. These studies may provide a foundation for developing therapeutics for clinical rabies, such as medication that could be used to enhance BBB permeability.

Rabies virus (RABV) is a negative-stranded RNA virus belonging to the genus *Lyssavirus* within the family *Rhabdoviridae* (1–3). RABV causes fatal encephalomyelitis resulting in more than 55,000 human deaths annually (2, 4). RABV enters neurons in the periphery at the wound site and then travels to the central nervous system (CNS) via sensory and motor neurons. Despite the dramatic clinical symptoms and outcome, surprisingly little tissue damage or neuronal pathology has been observed in the brains of rabid patients (5). In the mouse model, inflammation is mild after infection with wild-type (wt) RABV (6). However, extensive inflammation, apoptosis, and expression of innate immune genes have been found in the CNSs of mice infected with laboratory-attenuated RABV (7–12). Recently, it has been found that blood-brain barrier (BBB) permeability is enhanced in mice infected with laboratory-attenuated, but not wt, RABV (10, 13). Enhancement of BBB permeability is important in RABV attenuation by allowing immune effectors to enter the CNS and clear RABV (6, 10, 14). Therefore, enhancement of BBB permeability by using a disease model (experimental autoimmune encephalomyelitis [EAE]) (15, 16), as well as by administering laboratory-attenuated RABV, recombinant RABVs expressing three copies of the glycoprotein (G) (17), or immune-stimulating agents (18), resulted in clearing of wt RABV from the CNS and prevention of the development of rabies in mice.

The BBB is nonfenestrated to large molecules or xenobiotics, thus providing protection against the invasion of the CNS by macromolecules and microorganisms (19). The BBB is composed of endothelial cells (ECs), pericytes, and astrocytes (20). Alteration

Received 25 October 2013 **Accepted** 5 February 2014
Published ahead of print 12 February 2014
Editor: B. Williams
Address correspondence to Zhen F. Fu, zhenfu@uga.edu.
Q.C. and W.Q.H. contributed equally to this article.

doi:10.1128/JVI.03149-13

of BBB permeability is observed in both bacterial and viral infections. One of the key mechanisms of BBB breakdown is damage to the tight junction (TJ) in the brain microvascular ECs (BMECs) (19). The TJ complex is composed of both transmembrane TJ proteins (occludin and claudins) and cytosolic TJ proteins (zonula occludens-1 [ZO-1]) that link transmembrane TJ proteins to the actin cytoskeleton (21–23). Many viral infections, such as infections with human immunodeficiency virus (HIV), Japanese encephalitis virus (JEV), and mouse adenovirus type 1 (MAV-1), trigger changes in BBB permeability (24–26). Some of the viruses (for instance, MAV-1) enhance BBB permeability by direct disruption of the TJ complex in primary ECs (26), while others (for example, HIV) disrupt the TJ complex and enhance BBB permeability via induction of the expression of chemokines (particularly CCL2) in the CNS (24). In the EAE model, disruption of the BBB is associated with the infiltration of T-helper cells (27) and the production of interleukin 17A (IL-17A). IL-17A in T-helper 17 cell-signaling pathways has been demonstrated to induce the downregulation of TJ proteins and the influx of immune cells in C57BL/6 mice (28, 29). In the present study, the mechanism by which RABVs enhance BBB permeability was investigated, and it was found that the enhancement of BBB permeability and the reduction of TJ protein expression are associated not with direct RABV infection but rather with the expression of chemokines/cytokines after infection with laboratory-attenuated RABV.

MATERIALS AND METHODS

Cells, viruses, antibodies, and mice. Mouse brain microvascular ECs (bEnd.3) were obtained from the American Type Culture Collection (ATCC; Manassas, VA) and were maintained in Dulbecco's modified Eagle's medium (DMEM) supplemented with fetal bovine serum (FBS; ATCC). A human brain microvascular EC (hBMEC) line was obtained from Jason Zastre of the College of Pharmacy, University of Georgia. Mouse neuroblastoma (mNA) cells were maintained in RPMI 1640 medium (Mediatech, Herndon, VA) supplemented with 10% FBS. DRV-Mexico is a wt virus that originated from a Mexican dog and was propagated in suckling mouse brain (30). CVS-B2c is a RABV that was attenuated in the laboratory by passaging the challenge virus standard (CVS-24) in baby hamster kidney (BHK21) cells (31). The recombinant virus HEP-CXCL10 (rHEP-CXCL10) was constructed in our laboratory previously (7). A fluorescein isothiocyanate (FITC)-conjugated anti-RABV nucleoprotein antibody was obtained from Fujirebio (Malvern, PA). Rabbit polyclonal anti-occludin and anti-actin antibodies were obtained from Santa Cruz Biotechnology (Santa Cruz, CA). An antibody against gamma interferon (IFN-γ) (antibody XMG1.2) and a mouse IgG1 isotype control antibody were purchased from Thermo Scientific (Suwanee, GA). A rabbit polyclonal anti-claudin-5 antibody, a biotinylated goat anti-rabbit antibody, and an Alexa Fluor 488-conjugated goat anti-rabbit antibody were purchased from Invitrogen (Grand Island, NY). Mouse monoclonal anti-ZO-1 and rabbit polyclonal anti-CD3 antibodies were obtained from Sigma (St. Louis, MO) and Abcam (Cambridge, MA), respectively. Female ICR mice (4 to 6 weeks old) were purchased from Harlan and were housed in the animal facility in the College of Veterinary Medicine, University of Georgia. All animal experiments were carried out under protocols approved by the Institutional Animal Care and Use Committee (animal welfare assurance no. A3058-01).

Measurement of BBB permeability. BBB permeability was determined by measuring sodium fluorescein (NaF) uptake as described previously (32). Briefly, NaF was used as the tracer; 100 μl of 100-mg/ml NaF was injected into each mouse through the tail vein. Peripheral blood was collected after circulation for 10 min, and phosphate-buffered saline (PBS)-perfused brains were then harvested. The serum recovered was mixed with an equal volume of 10% trichloroacetic acid (TCA) and was then centrifuged for 10 min. The supernatant was collected after centrifugation and was made up to 150 μl by mixing with 5 M NaOH and 7.5% TCA. Homogenized brain samples in cold 7.5% TCA were centrifuged for 10 min at 10,000 × *g* to remove debris. The supernatant was made up to 150 μl by addition of 5 M NaOH. The fluorescence of serum and brain homogenate samples was measured using a spectrophotometer (BioTek Instruments, VT) with excitation at 485 nm and emission at 530 nm. The amount of NaF taken up into brain tissues is expressed as micrograms of fluorescence per milligram of cerebrum or cerebellum, divided by the micrograms of fluorescence per microliter of serum in order to normalize for the amounts of tracer taken up from peripheral blood at the time of brain tissue collection (32, 33). Data are expressed as the fold difference between the amount of tracer in tissues from virus-infected mice and the amount in tissues from the negative control.

Histopathology, IHC, and quantitative Western blot (WB) analysis. For histopathology and immunohistochemistry (IHC), infected mice were anesthetized with ketamine-xylazine (0.1 ml/10 g body weight) and were perfused with PBS followed by 10% neutral buffered formalin as described previously (12, 34). Three independent samples of mouse brains were harvested from each group. Brain tissues were removed and were paraffin embedded for coronal sections (thickness, 4 μm). The sections were stained with hematoxylin and eosin (HE) for histopathology. For IHC, the sections were deparaffinized and were rehydrated in xylene and ethanol. Endogenous peroxidase was quenched by incubation in 5% hydrogen peroxide, and antigens were retrieved in citrate buffer (Fisher Scientific, NH). The sections were then blocked with goat serum, incubated with primary antibodies overnight at 4°C, and then incubated with biotinylated secondary antibodies. The avidin-biotin-peroxidase complex (VectaStain Standard ABC kit; Vector Laboratories, Burlingame, CA) was used to localize the biotinylated antibody. Diaminobenzidine (DAB; Vector Laboratories) was utilized for color development. A negative control was performed by replacing primary antibodies with PBS. For antigen quantification, sections were photographed and analyzed using an Olympus (Tokyo, Japan) BX41 microscope. The integrated optical densities (IODs) of DAB signals were determined by Image-Pro Plus software (version 4.5; Media Cybernetics, Bethesda, MD).

For WB, three independent samples of mouse brains from each group were collected, homogenized, and prepared as 10% (wt/vol) suspensions in DMEM. After centrifugation, the supernatants were collected and stored at −80°C. The brain extracts or cell lysates were subjected to 8% to 16% sodium dodecyl sulfate-polyacrylamide gel electrophoresis (SDS-PAGE) (Thermo Scientific, Rockford, IL). Separated proteins were electroblotted onto nitrocellulose membranes and were incubated with primary antibodies overnight. After extensive washing with PBS, the blots were incubated with secondary antibodies. Proteins were detected by SuperSignal West Pico chemiluminescence (Thermo Scientific). Band signals corresponding to immunoreactive proteins were captured, and chemiluminescence intensities were analyzed, using a ChemiDoc 4000 MP documentation system (Bio-Rad, CA).

Infection of BMECs with RABV and detection of viral antigen and RNA. Monolayers of bEnd.3 cells or hBMECs in six-well plates were cocultured with RABV at a multiplicity of infection (MOI) of 1. Viruses were seeded and incubated with the cells for 1 h at 37°C, and then the cells were washed three times with PBS (35). The plates were refilled with fresh medium and were incubated at 34°C for 24, 48, and 120 h. mNA cells infected with RABVs were included as positive controls. Virus antigen was detected by a direct fluorescent-antibody (dFA) assay as described previously (36). Acetone-fixed cells were stained with an FITC-conjugated anti-RABV N antibody. Antigen-positive foci were captured under a fluorescence microscope (Zeiss, Germany). All experiments were carried out in quadruplicate. Viral RNA in BMECs was detected by using quantitative reverse transcription-PCR (qRT-PCR). RNA was extracted from BMECs infected with RABV by using the RNAeasy Minikit (Qiagen, Germany). Total RNA was reverse transcribed into cDNA by using the SuperScript III first-strand synthesis system for RT-PCR (Invitrogen, NY) according to

the manufacturer's instructions. Real-time quantitative PCR was performed using the Brilliant II SYBR green QRT-PCR master mix kit (Agilent Technologies, CA). The following set of primers was used: forward, 5′GGAAAAGGGACATTTGAAAGAA3′; reverse, 5′AGTCCTCGTCATC AGAGTTGAC3′. Gene expression was analyzed in an Mx3000P apparatus (Stratagene, La Jolla, CA).

Confocal microscopy. RABV was seeded on monolayers of bEnd.3 cells at an MOI of 1 for 24 h at 37°C on coverslips, and cells were fixed with 4% paraformaldehyde and were stained with antibodies to TJ proteins. In addition, a 10% (wt/vol) suspension of brain extract was prepared by homogenizing brain tissues in DMEM containing Complete proteinase inhibitor cocktail (Roche, Germany). Brain homogenates were centrifuged to remove debris, and supernatants were harvested and were seeded onto monolayers of bEnd.3 cells for 24 h. Cells were fixed and were permeabilized with 0.2% Triton X-100. The expression of TJ protein was detected by using primary anti-occludin or anti-claudin-5 antibodies. After washing, cells were incubated with an Alexa Fluor 488-conjugated goat anti-rabbit secondary antibody for 1 h at room temperature. Samples were mounted using Prolong Gold antifade reagent with DAPI (4′,6-diamidino-2-phenylindole) (Invitrogen, NY) and were visualized with a Nikon A1 confocal laser microscope system equipped with NIS-Elements imaging software (version 4.13; Nikon Instruments, Inc., Melville, NY). The images recorded were quantified using NIH's Fiji (downloaded from pacific.mpi-cbg.de/wiki/index.php/fiji), a distribution package of ImageJ. The mean fluorescence intensity (MFI) is calculated using the region of interest (ROI), which is drawn around an entire cell so that it always includes the membrane. Three independent experiments were carried out for each condition. Background staining was accounted for by using three negatively stained regions per cell, which were subtracted from the total mean fluorescence.

Determination of cytokine expression in brain extracts. Extracts from homogenized brains were analyzed simultaneously for concentrations of 30 mouse chemokines/cytokines by using the Milliplex MAP 30-plex premixed mouse cytokine/chemokine magnetic bead panel (Millipore, Billerica, MA) (37) according to the manufacturer's instructions. The 30 cytokines and chemokines analyzed included colony-stimulating factor 1 (CSF1), CSF3, vascular endothelial growth factor (VEGF), leukemia inhibitory factor (LIF), CSF2, tumor necrosis factor alpha (TNF-α), IL-1α, IL-2, IL-3, IL-4, IL-5, IL-6, IL-7, IL-10, IL-12p40, IL-12p70, IL-13, IL-15, IL-17, IFN-γ, C-C motif ligand 2 (CCL2), CCL3, CCL4, CCL5, CCL11, C-X-C motif ligand 1 (CXCL1), CXCL2, CXCL9, CXCL10, and CXCL5. Premixed magnetic beads conjugated to antibodies for all 30 analytes were mixed with equal volumes of brain extracts in 96-well plates. Plates were protected from light and were incubated on an orbital shaker overnight at 4°C, and magnetic beads were washed with 200 μl of wash buffer three times. Then detection antibodies were added to each well, and the mixtures were incubated at room temperature for 1 h. Streptavidin-phycoerythrin was added to each well, and the mixtures were incubated at room temperature for 30 min. The magnetic beads were resuspended in sheath fluid, and plates were assayed on a Magpix system with xPONENT software. Median fluorescence intensity data were analyzed using a 5-parameter logistic method for calculating cytokine/chemokine concentrations in brain homogenates.

IPA. The differentially expressed gene list (Luminex) was loaded into Ingenuity pathway analysis (IPA) software (version 5.0) in order to perform biological network and functional analyses. IPA is a Web-based software application containing most of the knowledge of biological interactions between gene products in the literature. When one uses the IPA software, the networks obtained describe functional relationships between gene products based on known interactions in the literature. The IPA tool then associates these networks with known biological functions and canonical pathways. Canonical pathway analysis identifies the pathways from the IPA library that are most significant to the data set.

Statistical analysis. Data are expressed as means ± standard errors of the means (SEM), and the significance of differences between groups was evaluated by Student's *t* test or by one-way analysis of variance (ANOVA) followed by Tukey's *post hoc* tests. Graphs were plotted and analyzed using GraphPad Prism, version 5.0 (GraphPad Software, La Jolla, CA).

RESULTS

Laboratory-attenuated RABV enhanced BBB permeability more than wt RABV. Previous studies demonstrated that laboratory-attenuated CVS-B2c, but not wt DRV-Mexico, enhanced BBB permeability via intramuscular infection (6). To investigate if intracranial (i.c.) infection with either of the viruses (DRV-Mexico or CVS-B2c) induces similar changes in BBB permeability, the leakage of NaF from the peripheral circulation into the CNS was measured in the cerebra or cerebella of mice infected with either of the viruses. At day 6 postinfection (p.i.), the BBB was found to be significantly more permeable in the cerebra of mice infected with 10 $MICLD_{50}$ (mouse intracerebral 50% lethal doses) of CVS-B2c (>3-fold increase in NaF uptake) than in those infected with DRV-Mexico (almost no change), even when 10 times more virus was used (100 LD_{50} of DRV-Mexico) (Fig. 1A). No significant difference was detected in the BBB permeability change in the cerebellum at this time point. By day 9 p.i., BBB permeability in the cerebra of mice infected with CVS-B2c continued to be enhanced (>4-fold increase in NaF uptake). The most significant BBB permeability enhancement was observed in the cerebella of mice infected with 10 LD_{50} CVS-B2c (>7-fold increase in NaF uptake) at day 9 p.i. (Fig. 1A). At this time point, NaF uptake was 2- to 4-fold increased in the cerebella of mice infected with DRV-Mexico, indicating that BBB permeability was not increased until the end of the disease process in mice infected with wt RABV (at day 9 p.i., almost all animals had developed severe disease and reached the humane point for euthanasia). Overall, BBB permeability in the CNS was significantly more enhanced in mice infected with CVS-B2c than in those infected with DRV-Mexico (P, <0.05).

Laboratory-attenuated RABV induced more infiltration of inflammatory cells into the CNS than wt RABV. To investigate the effects of the enhancement of BBB permeability on cell infiltration, mice were infected with each of the RABVs, and the brains were harvested and stained with HE. Perivascular cuffing and neuronal degeneration were observed in the brains of mice infected with CVS-B2c at days 6 and 9 p.i., while only a few cells had accumulated in the perivascular spaces of mice infected with DRV-Mexico by day 6 p.i. (Fig. 1C). It has been demonstrated that $CD4^+$ T cells are required for the enhancement of BBB permeability in RABV infection (32). To quantify infiltrating T cells, CD3 was chosen as the T cell marker. Brain sections were stained with anti-CD3 antibodies, and the numbers of $CD3^+$ T cells were estimated. As shown in Fig. 1C, $CD3^+$ T cells were seen surrounding the blood vessels of mice inoculated with a low dose of CVS-B2c or invading the parenchymas of mice infected with a high dose of CVS-B2c at day 6 p.i., but only mice infected with a high dose of CVS-B2c showed significantly more $CD3^+$ T cells than the control (Fig. 1B). Almost no $CD3^+$ T cells were seen in mice infected with DRV-Mexico at this time point. By day 9 p.i., significantly more $CD3^+$ T cells were seen surrounding blood vessels and in the parenchymas of mice infected with both low and high doses of CVS-B2c than in the control (Fig. 1C). Few $CD3^+$ T cells were observed in mice infected with a low dose of DRV-Mexico, while more $CD3^+$ T cells surrounding the vessels were observed in mice infected with a high dose of DRV-Mexico (Fig. 1B and C). Overall,

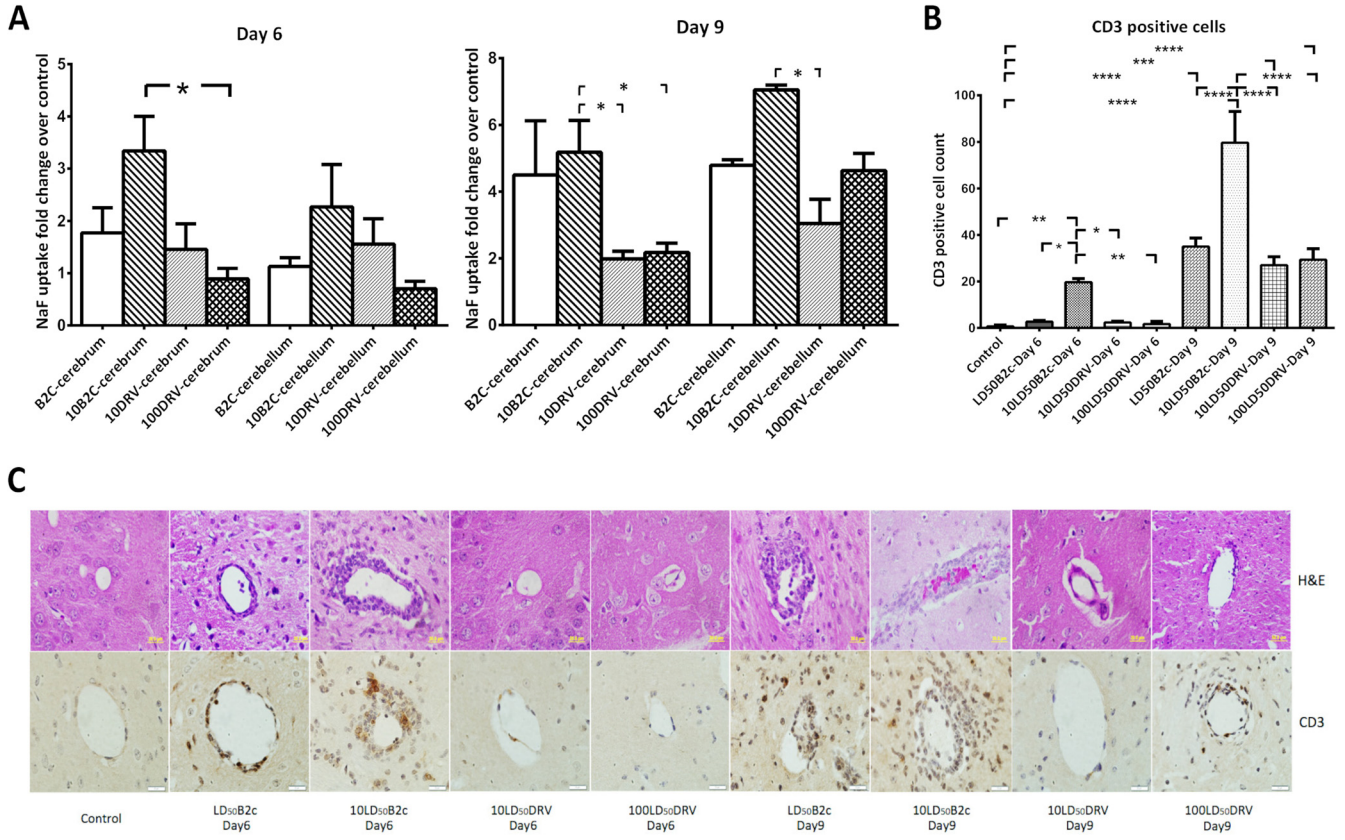

FIG 1 NaF uptake and inflammatory cell infiltration in the CNSs of mice infected with laboratory-attenuated CVS-B2c or wt DRV-Mexico. Female ICR mice were infected i.c. either with 1 or 10 LD_{50} of CVS-B2c or with 10 or 100 LD_{50} of DRV-Mexico. (A) At day 6 or 9 p.i., BBB permeability was assessed by NaF uptake in the cerebrum and the cerebellum. (B) $CD3^+$ T cells were quantified and analyzed statistically. Data are means ± SEM of results from three independent experiments. Statistical analyses for panels A and B were performed using one-way ANOVA followed by Tukey's *post hoc* test. Asterisks indicate statistical significance (*, $P < 0.05$; **, $P < 0.01$; ***, $P < 0.001$; ****, $P < 0.0001$). (C) Harvested brains were subjected to HE staining for histopathology as well as to IHC for the detection of $CD3^+$ T cells.

significantly more infiltrated T cells were detected in the CNSs of mice infected with CVS-B2c than in those infected with DRV-Mexico ($P < 0.01$) (Fig. 1B).

Laboratory-attenuated RABV reduced TJ protein expression in the CNS more than wt RABV. To provide insight into the mechanisms by which laboratory-attenuated RABV enhances BBB permeability, the expression levels of TJ proteins (claudin-5, occludin, and ZO-1) in the brains of mice infected with CVS-B2c or DRV-Mexico were assessed by IHC and quantitative WB using antibodies to each of the TJ proteins. The immune reactivities of the transmembrane TJ proteins claudin-5 and occludin in the brains of mice infected with DRV-Mexico were similar to those in the brains of sham-infected mice, while staining of occludin and claudin-5 was partially lost in the brains of mice infected with CVS-B2c at day 6 p.i. (Fig. 2A). The integrated optical densities (IODs) of both occludin and claudin-5 staining were significantly lower in the brains of mice infected with CVS-B2c than in the brains of sham-infected mice or mice infected with DRV-Mexico at day 6 p.i. The reductions were even more dramatic in mice infected with CVS-B2c by day 9 p.i. (Fig. 2B). Likewise, the pattern of cytoplasmic TJ protein ZO-1 in the brains of mice infected with DRV-Mexico was similar to that in sham-infected mice at day 6 p.i., while the expression level of ZO-1 in mice infected with CVS-B2c was significantly diminished at day 6 p.i. (P, <0.01). Overall, in mice infected with CVS-B2c, the expression levels of ZO-1, occludin, and claudin-5 at day 9 p.i. were reduced to 3.04%, 5.47%, and 6.34% of the levels in sham-infected mice, respectively (Fig. 2B). The IHC data were confirmed by WB (Fig. 2C). The expression levels of TJ proteins were significantly lower in mice infected with CVS-B2c (particularly in mice infected with a high dose at day 9 p.i.) than in sham-infected mice or in mice infected with DRV-Mexico (Fig. 2D). By day 9 p.i., the expression of TJ proteins in mice infected with DRV-Mexico was slightly decreased, corresponding to the increased BBB permeability, particularly in the cerebella of mice infected with the higher dose of DRV-Mexico. These results indicate that the TJ complex is broken down in mice infected with laboratory-attenuated CVS-B2c.

Neither laboratory-attenuated nor wt RABV infects BMECs or affects the expression of TJ proteins in BMECs. To determine whether laboratory-attenuated RABV infection causes direct damage to BMECs, laboratory-attenuated CVS-B2c or wt DRV-Mexico was inoculated onto human or mouse BMECs at an MOI of 1. mNA cells were infected with each virus as positive controls. As shown in Fig. 3A, both RABVs replicated productively in mNA cells as demonstrated by viral antigen staining. No RABV antigen was detectable in the monolayers of hBMECs or bEnd.3 cells, indicating that neither DRV-Mexico nor CVS-B2c infects BMECs (Fig. 3A). Phase-contrast microscopy showed that bEnd.3 cells and hBMECs were viable at this

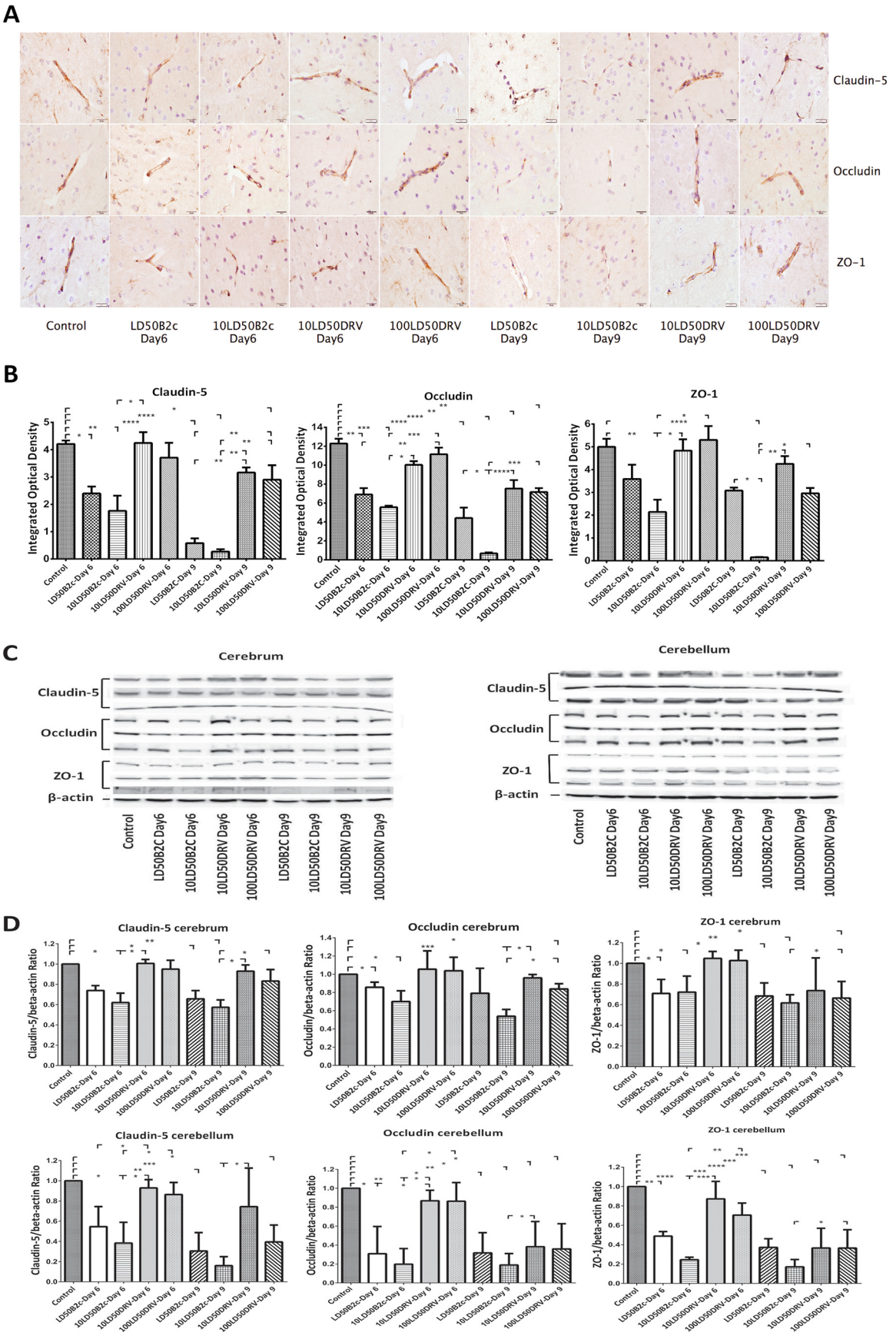
A
Claudin-5
Occludin
ZO-1
Control
LD50B2c Day6
10LD50B2c Day6
10LD50DRV Day6
100LD50DRV Day6
LD50B2c Day9
10LD50B2c Day9
10LD50DRV Day9
100LD50DRV Day9
B
Claudin-5
Occludin
ZO-1
Integrated Optical Density
C
Cerebrum
Cerebellum
Claudin-5
Occludin
ZO-1
β-actin
D
Claudin-5 cerebrum
Occludin cerebrum
ZO-1 cerebrum
Claudin-5 cerebellum
Occludin cerebellum
ZO-1 cerebellum
Claudin-5/beta-actin Ratio
Occludin/beta-actin Ratio
ZO-1/beta-actin Ratio

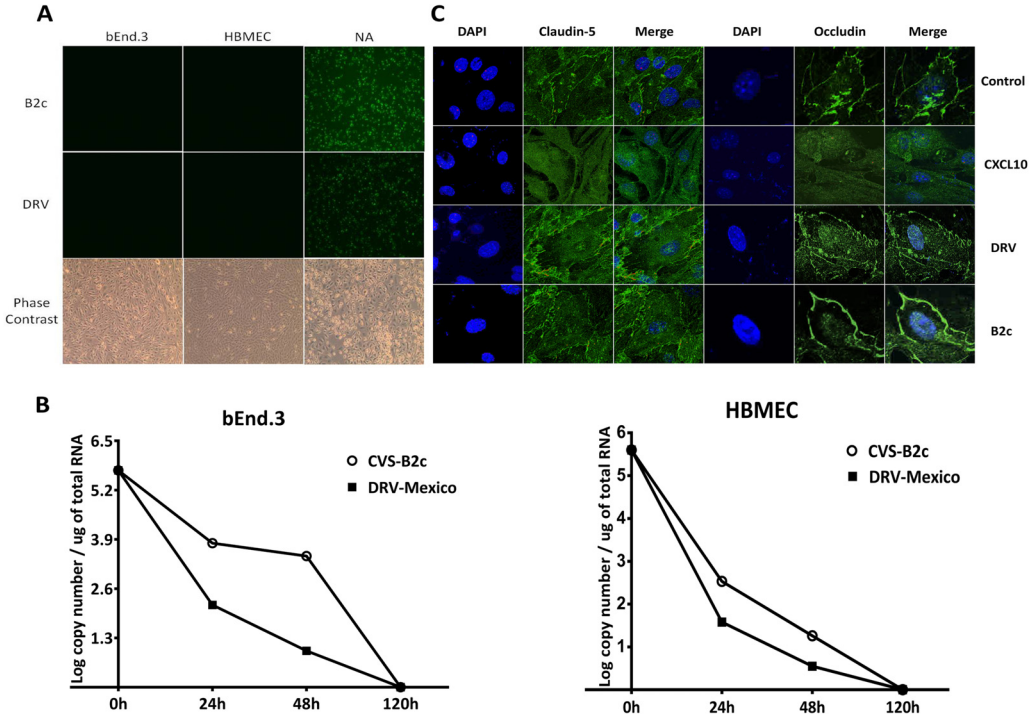

FIG 3 Infection of human or mouse BMECs with RABVs and their effects on TJ protein expression. (A) Human or mouse BMECs were cocultured with CVS-B2c or DRV-Mexico at an MOI of 1, and cells were fixed at 120 h after inoculation to assess active viral replication by using FITC-conjugated anti-RABV N antibodies. mNA cells infected with each virus were included as positive controls. Phase-contrast microscopy was performed to ensure cell viability and structure. (B) Viral RNA from mouse or human BMECs infected with each virus was detected at 0, 24, 48, and 120 h by quantitative RT-PCR. (C) The expression of TJ proteins on BMECs cocultured with either virus was detected by using confocal microscopy and antibodies to TJ proteins. BMECs cocultured with the supernatant of mNA cells infected with rHEP-CXCL10 were included as a positive control.

time. To confirm this finding, viral RNA was detected by quantitative RT-PCR (Fig. 3B). Viral RNA levels in the culture decreased by 24 and 48 h p.i. and became undetectable by 120 h p.i., indicating the lack of active virus replication in the infected cells.

The expression levels of TJ proteins in RABV-infected BMECs were also investigated. No significant difference in the expression of occludin or claudin-5 was found between sham-treated bEnd.3 cells and cells inoculated with either RABV (Fig. 3C). Since previous studies had shown that infection with a recombinant RABV expressing CXCL10 (rHEP-CXCL10) enhanced BBB permeability (7), the supernatant from mNA cells infected with rHEP-CXCL10 (containing a high concentration of CXCL10) was inoculated with bEnd.3 cells for 24 h. As shown in Fig. 3C, the expression of occludin and claudin-5 decreased to undetectable levels. These results suggest that RABV does not infect BMECs and that the loss of TJ protein expression is not due directly to RABV infection.

TJ protein expression in BMECs was altered by extracts from the brains of mice infected with laboratory-attenuated RABV. Since direct RABV inoculation does not alter the expression of TJ proteins in BMECs, extracts from the brains of mice infected with either RABV were cocultured with bEnd.3 cells, and the expression levels of TJ proteins were assessed by confocal microscopy. As shown in Fig. 4A, strong peripheral patterns of claudin-5 and occludin were observed in cells treated with extracts from the brains of sham-infected mice. Similar patterns were also observed in cells treated with day 6 p.i. brain extracts from mice infected with DRV-Mexico, although the expression levels of occludin and claudin-5 were reduced at the peripheries of cells treated with day 9 p.i. brain extracts from mice infected with 100 LD_{50} DRV-Mexico (Fig. 4A). In contrast, the expression of TJ proteins was significantly decreased in cells treated with brain extracts prepared either at day 6 p.i. or at day 9 p.i. from mice infected with CVS-B2c (Fig. 4A and B). These observations were confirmed by quantitative Western blotting (Fig. 4C). The expression of TJ proteins (occludin and claudin-5) diminished almost completely in bEnd.3 cells treated with brain extracts prepared at day 9 p.i. from mice infected with CVS-B2c (Fig. 4D). Overall, these results indicate that the expression of TJ protein is downregulated by molecules in the

FIG 2 Expression of TJ proteins (claudin-5, occludin, and ZO-1) in the brains of mice infected with CVS-B2c or DRV-Mexico. Mice were infected i.c. either with 1 or 10 LD_{50} of CVS-B2c or with 10 or 100 LD_{50} of DRV-Mexico. (A) At day 6 or 9 p.i., animals were euthanized, and brains were harvested, fixed, and sectioned for measurement of the expression of TJ proteins using IHC with antibodies to the respective TJ proteins. (B) The expression levels of individual TJ proteins were estimated by quantifying IODs and were analyzed statistically. (C) The expression of TJ proteins in RABV-infected mouse brains was confirmed by Western blotting. (D) TJ protein expression as detected by Western blotting was quantitatively analyzed in brain extracts from mice infected with either virus (CVS-B2c or DRV-Mexico) or from sham-infected mice. Data are means ± SEM of results from three independent experiments. Statistical significance in panels B and D was assessed using one-way ANOVA followed by Tukey's *post hoc* test. Asterisks indicate statistical significance (*, $P < 0.05$; **, $P < 0.01$; ***, $P < 0.001$; ****, $P < 0.0001$).

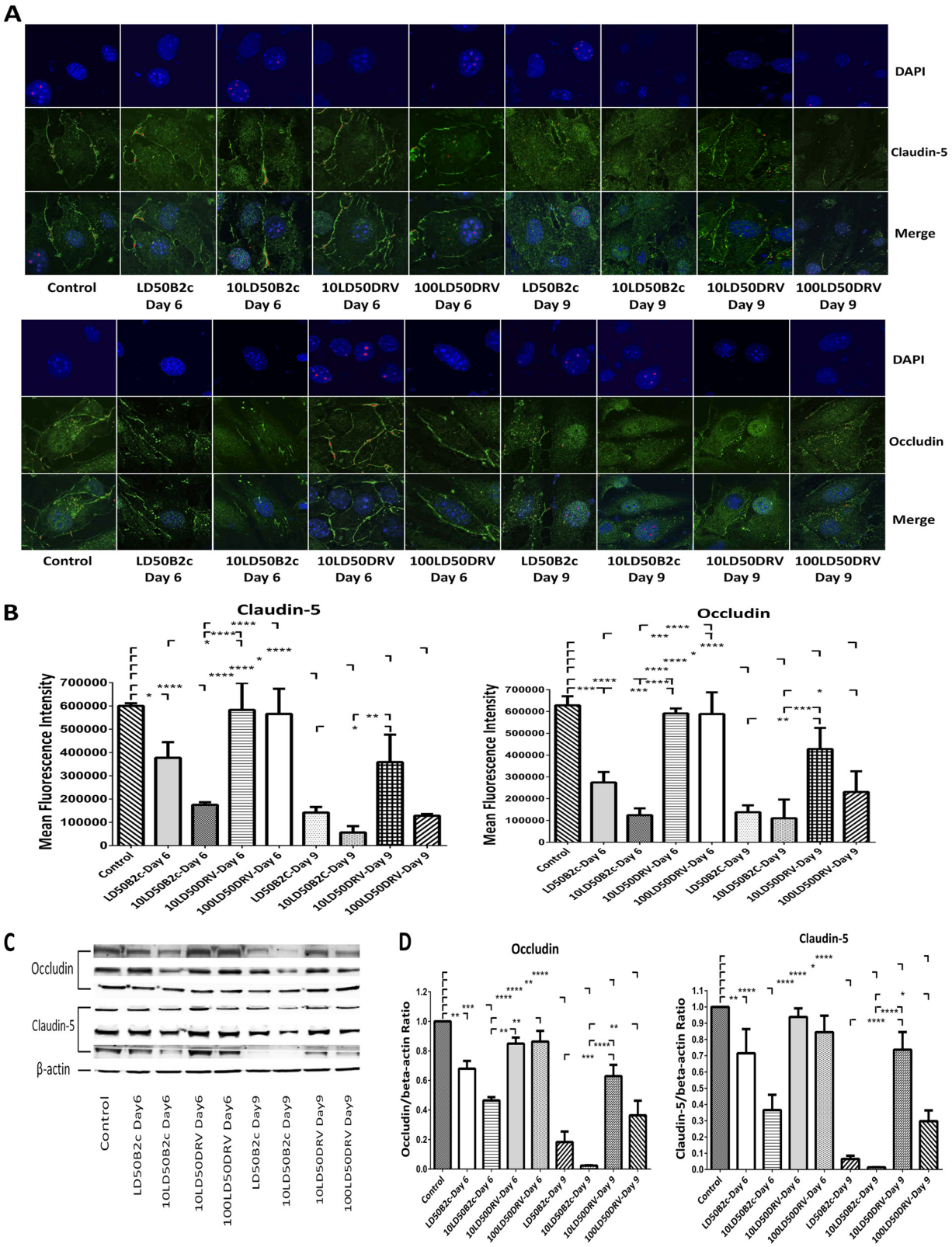

FIG 4 Effects of brain extracts derived from mice infected with CVS-B2c or DRV-Mexico on the expression of TJ proteins in BMECs. (A) Mouse BMECs were cocultured with brain extracts from mice infected with different doses of CVS-B2c or DRV-Mexico. After 24 h, BMECs were fixed and were stained with DAPI and an anti-claudin-5 antibody or with DAPI and an anti-occludin antibody. The staining was visualized by confocal microscopy. (B) MFI for the ROI drawn around the cells and statistical analysis. (C) The expression of TJ proteins in BMECs after coculturing with brain extracts was also detected using Western blotting. (D) TJ protein expression as detected by WB was quantitatively analyzed in BMECs treated with brain extracts from mice infected with either virus (CVS-B2c or DRV-Mexico). bEnd.3 cells treated with brain extracts from sham-infected mice were included as controls. Data are means ± SEM of results from three independent experiments. Statistical analyses in panels B and D were performed with one-way ANOVA followed by Tukey's *post hoc* test. Asterisks indicate statistical significance (*, $P < 0.05$; **, $P < 0.01$; ***, $P < 0.001$; ****, $P < 0.0001$). Three samples were collected from three replicates in each group for statistical analysis.

brain extracts from mice infected with laboratory-attenuated RABV.

Cytokine profiling showed significantly more elevated chemokines/cytokines in the brain extracts of mice infected with laboratory-attenuated RABV than in those of mice infected with wt RABV. To analyze the expression of chemokines/cytokines in the brain extracts that might be responsible for the reduction of TJ protein expression in BMECs, cytokine profiling was performed using the Milliplex MAP 30-plex premixed mouse cytokine/chemokine magnetic bead panel. This panel was chosen because it contains antibodies to the chemokines/cytokines previously determined to be differentially regulated by laboratory-attenuated and wt RABV (10). As shown in Fig. 5, 25 out of 30 chemokines/cytokines were produced at significantly higher levels in the brains of mice infected with CVS-B2c than in those of mice infected with DRV-Mexico (Fig. 5). These include chemokines (CXCL10, CXCL9, CXCL2, CXCL1, CCL11, CCL5, CCL4, CCL3, and CCL2), interleukins (IL-1α, IL-17, IL-13, IL-12, IL-7, IL-6, and IL-5), and growth factors (VEGF, CSF3, CSF2, CSF1, and LIF). Most of these cytokines were upregulated by day 6 p.i. and continued to increase by day 9 p.i., while others (CXCL2, IFN-γ, CSF1, and LIF) were upregulated only by day 9 p.i., indicating that they might be induced by other cytokines at a later point in infection. The increase in the expression of CXCL10 was so great that it was out of the detection range in the brain extracts prepared from mice infected with CVS-B2c. The production of cytokines involved in the Th1 signaling pathway, such as IFN-γ and IL-12, was significantly elevated in mice infected with CVS-B2c, while the secretion of IL-4 and IL-10, involved in the Th2 signaling pathway, remained unchanged in all groups.

Molecular network analysis of differentially expressed genes in the CNSs of mice exposed to RABV. Luminex data were further analyzed with IPA in order to map the networks of chemokines/cytokines expressed in the brains of mice infected with CVS-B2c or DRV-Mexico. Chemokines/cytokines were mapped into genetic networks with related molecules in different signaling pathways in the IPA database, and the pathways were ranked by scores. The higher a score, the lower the chance that a network is achieved by random chance alone. Our analysis generated a CVS-B2c network with a score of 59 and a DRV-Mexico network with a score of 26. These pathways contain 26 and 12 focus molecules, respectively. In the molecular network generated from the group of mice infected with CVS-B2c, IFN-γ is located in the center and is directly linked with CXCL10, CXCL9, CCL5, IL-17, IL-12, IL-6, and VEGF (Fig. 6A). In contrast, TNF-α is located in the center of the network generated from mice infected with DRV-Mexico and connects with CCL11 and CXCL10 (Fig. 6B).

Neutralization of IFN-γ ameliorated the disruption of BBB integrity and the downregulation of TJ proteins. The IPA data described above indicate that IFN-γ is located in the center of a molecular network that could play an important role in the enhancement of BBB permeability during infection with laboratory-attenuated RABV. To investigate if disruption of IFN-γ function inhibits the enhancement of BBB permeability, mice were infected with laboratory-attenuated RABV and were treated with anti-IFN-γ neutralizing antibodies intraperitoneally (i.p.) at days 0, 2, and 4 after infection. NaF uptake was measured at day 6 p.i. An isotype control antibody was included. As shown in Fig. 7A, treatment with an anti-IFN-γ antibody significantly decreased the enhancement of BBB permeability observed for treatment with isotype control antibodies both in the cerebrum and in the cerebellum. To test if the anti-IFN-γ antibody blocks the downregulation of TJ protein expression, bEnd.3 cells were treated with a mixture of an anti-IFN-γ antibody and a brain extract prepared from mice infected with CVS-B2c (10 LD_{50}). It was found that the expression of claudin-5 and occludin in cells treated with the mixture of the anti-IFN-γ antibody and the mouse brain extract was indistinguishable from that for isotype control antibody-treated cells (Fig. 7B and C). The expression of claudin-5 and occludin was significantly higher in cells inoculated with the brain extract mixed with the anti-IFN-γ antibody than in cells treated with the brain extract mixed with an isotype control antibody (Fig. 7B and C). These results suggest that IFN-γ is a critical mediator of BBB permeability enhancement and TJ protein expression after infection with laboratory-attenuated RABV.

DISCUSSION

The BBB is a physical and physiological barrier against the entry of cells and molecules into the CNS (20, 22, 23), and thus, enhancement of BBB permeability has often been associated with pathological changes in the CNS (19). However, transiently increased BBB permeability has been associated with the clearance of RABV from the CNS and the prevention of rabies (13). Laboratory-attenuated and recombinant RABVs (17, 18) can transiently enhance BBB permeability in a mouse model as early as day 6 after infection. On the other hand, wt RABV does not induce the enhancement of BBB permeability (6, 10, 13). Since TJ proteins are important in maintaining BBB integrity, TJ protein expression was investigated *in vitro* and *in vivo* after intracranial infection with laboratory-attenuated or wt RABV in the present study. The expression levels of TJ proteins were found to be reduced in the brains of mice infected with laboratory-attenuated, but not wt, RABV. Furthermore, *in vitro* studies with BMECs indicate that the reduction in the level of TJ protein expression is caused not by RABV infection *per se* but by chemokines/cytokines induced after infection with laboratory-attenuated RABV.

ECs are the major components of the BBB, and TJ proteins present on and between the ECs form a barrier that maintains the homeostasis of the CNS by restricting the diffusion of blood-borne molecules (38). Alteration of TJ protein expression has been observed in viral infections (MAV-1) or autoimmune diseases (EAE) (26, 28). The levels of ZO-2, claudin-5, and occludin mRNAs and proteins are reduced in ECs infected with MAV-1 (26). In EAE, both claudin-5 and occludin are downregulated, and claudin-5 has been shown to be the key determinant for BBB breakdown (39). Reductions in TJ protein levels at the impaired BBB and the influx of encephalitogenic T cells generate plaques in the brain parenchyma, resulting in the exacerbation of EAE (40). However, enhanced BBB permeability has been shown to be beneficial for RABV infection, since a permeable BBB allows immune effectors to enter the CNS and clear RABV from the CNS (7, 10). In the present study, the mechanisms by which laboratory-attenuated RABV enhances BBB permeability were investigated, and significantly decreased expression of TJ proteins (claudin-5, occludin, and ZO-1) was observed in mice infected with laboratory-attenuated RABV, corresponding to the enhancement of BBB permeability in these animals. Little to no reduction in the level of TJ protein expression was found in the brains of mice infected with wt RABV, and no enhancement of BBB permeability was found in these animals until the end stage of disease. Reductions in the

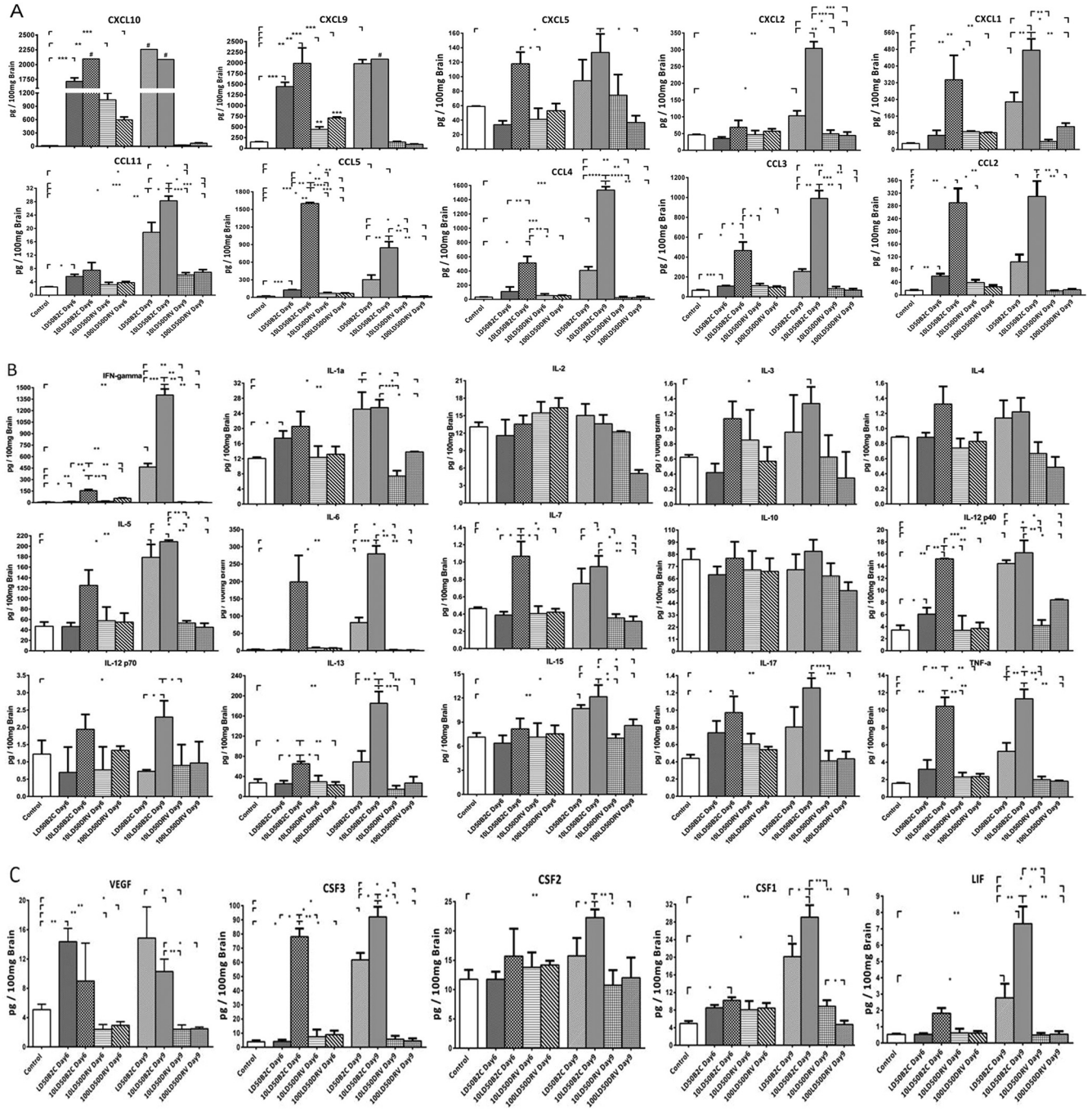

FIG 5 Measurement by Luminex assay of cytokines in brain extracts from mice infected with CVS-B2c or DRV-Mexico. ICR mice were infected i.c. either with 1 or 10 LD_{50} of CVS-B2c or with 10 or 100 LD_{50} of DRV-Mexico. At day 6 or 9 p.i., animals were euthanized, and brains were harvested and homogenized. After centrifugation, the supernatants were loaded in order to measure the concentrations of the indicated cytokines by using the Luminex assay. Shown are expression levels of chemokines (A), interleukins, TNF-α, and IFN-γ (B), and growth factors (C). Experiments were performed with three replicates for each time point and condition. Hash tags indicate expression levels of cytokines beyond the upper detection range. Data are means ± SEM of results from three independent experiments. Statistical analyses were performed with one-way ANOVA followed by Tukey's *post hoc* test. Asterisks indicate statistical significance (*, $P < 0.05$; **, $P < 0.01$; ***, $P < 0.001$; ****, $P < 0.0001$).

levels of TJ protein expression have been reported recently for rats infected with RABV (41). However, only the expression of occludin, not that of ZO-1, was found to be reduced in infected animals. This discrepancy may have been due to the different animal models used. The LEW/SsNNarl rat used in the study of Liao et al. (41) is an inbred strain that may possess allelic loci impacting the severity of RABV in rats (42), while the ICR mouse used in the present study is an outbred strain that mimics the genetic diversity of the general population.

Many host and viral factors contribute to the disruption of BBB integrity (19). In HIV, alteration of occludin and ZO-1 expression at the BBB has been demonstrated to be dependent on viral gp120 and CCL2 (43–46). MAV-1 infects ECs and directly damages TJ proteins, so alteration of TJ proteins is cytokine independent (26). In EAE, IL-17 signaling is crucial for the reduction of TJ protein expression and the trafficking of encephalitogenic T cells to the brain (47, 48). Our data show that RABV does not infect human or mouse BMECs *in vitro* as

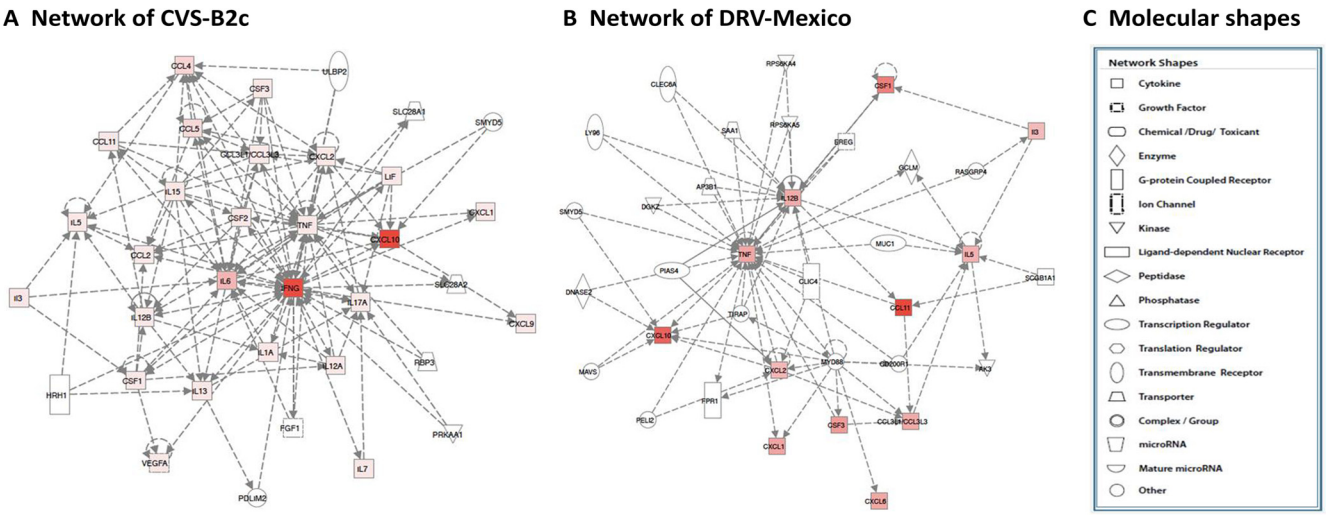

FIG 6 Ingenuity pathway analysis of the immune response, regulatory networks, and pathways mediated by infection with CVS-B2c or DRV-Mexico. Data generated by the Luminex assay were analyzed with IPA software. One network of genes expressed in the brains of mice infected with CVS-B2c (A) and one network of genes expressed in the CNSs of mice infected with DRV-Mexico (B) were established. Nodes represent genes; their shapes represent the functional classes of the gene products (C); and arrows indicate the biological relationships between the nodes. The intensity of the node color indicates the degree of upregulation (red) in mice inoculated with either RABV. White (noncolored) nodes are nonfocus genes that are biologically relevant to the pathways but were not identified as differentially expressed by our Luminex analysis.

detected by viral antigen expression or viral RNA replication. Likewise, RABV does not damage TJ proteins in these cells. To investigate what induced the reduction in TJ protein expression in RABV-infected mice, brain extracts were prepared from mice infected with laboratory-attenuated CVS-B2c or wt DRV-Mexico. The expression of claudin-5 and occludin decreased significantly in BMECs incubated with brain extracts derived from mice at day 6 or 9 after infection with laboratory-attenuated RABV, while the expression of TJ proteins showed some reduction only in BMECs cocultured with brain extracts prepared from mice at day 9 after infection with wt RABV. Therefore, the disruption of TJ proteins and the enhancement of BBB permeability are due not to direct RABV infection but to the molecules in the brain extracts induced by laboratory-attenuated RABV.

To analyze the molecules in the brain extracts induced by RABV infection that are associated with the reduction of TJ protein expression, a Milliplex MAP 30-plex premixed mouse cytokine/chemokine magnetic bead panel was used to measure the levels of chemokines/cytokines in the mouse brain. This panel was selected because previous studies have indicated that infection with attenuated RABV increased the expression of innate immune genes (6, 10). A recombinant RABV expressing a chemokine (CXCL10, CCL5, or CCL3) induced the enhancement of BBB permeability in mice (7) and reduced the expression of TJ proteins in BMECs, as shown in this study. Furthermore, enhancement of BBB permeability is chemokine/cytokine dependent in many diseases (19). For example, CCL2 has been demonstrated to reduce the expression of ZO-1, ZO-2, occludin, and claudin-5 in HIV-1-infected BMECs through Rho and Rho kinase signaling (49). In EAE, IL-17-induced reactive oxygen species activate myosin light-chain kinase and reduce expression levels of ZO-1 and occludin in BMECs (28). Indeed, our Luminex data showed that brain extracts from mice infected with laboratory-attenuated RABV contained significantly higher levels of chemokines/cytokines than those from mice infected with wt RABV. These include CXCL10, CXCL1, CCL11, CCL5, CCL4, CCL3, CCL2, IL-1α, IL-17, IL-12, IL-6, IL-5, and IFN-γ. These results suggest that these elevated levels of chemokines/cytokines could be responsible for the reduction of TJ protein expression and consequently for the enhancement of BBB permeability in mice infected with laboratory-attenuated RABV.

To decipher the pathway(s) by which chemokines/cytokines reduce the expression of TJ proteins, molecular networks associated with differentially expressed genes were analyzed in the present study. In mice infected with laboratory-attenuated RABV, IFN-γ is located in the center of the molecular network. It has been reported that IFN-γ, but not TNF-α, is associated with enhanced BBB permeability through the ONOO-dependent pathway in RABV infection (32). By neutralizing IFN-γ with antibodies, the enhancement of BBB permeability can be ameliorated in mice, and the expression of TJ proteins can be restored in BMECs, infected with laboratory-attenuated RABV. These studies further confirm that inflammatory cytokines/chemokines (particularly IFN-γ) play a central role in enhancing BBB permeability in mice infected with RABV by downregulating TJ protein expression. Pathway analysis also indicates that IFN-γ connects directly with the most highly expressed chemokine, CXCL10. Although only low levels of IFN-γ were detected at day 6 p.i., it is highly expressed at the later stage of infection (day 9 p.i.). Thus, CXCL10 could be the initiation factor for the reduction in TJ protein expression and the enhancement of BBB permeability in mice infected with laboratory-attenuated RABV. Recombinant RABV expressing CXCL10 also significantly enhanced BBB permeability, as shown in previous studies (7).The immunofluorescence data in our study showed substantial reductions in occludin and claudin-5 expression in BMECs incubated with a supernatant containing CXCL10. CXCL10 can be secreted by brain-resident cells such as neurons, microglial cells, and astrocytes (50, 51); it can also be produced by the infiltrating immune cells from the periphery (52). In West Nile

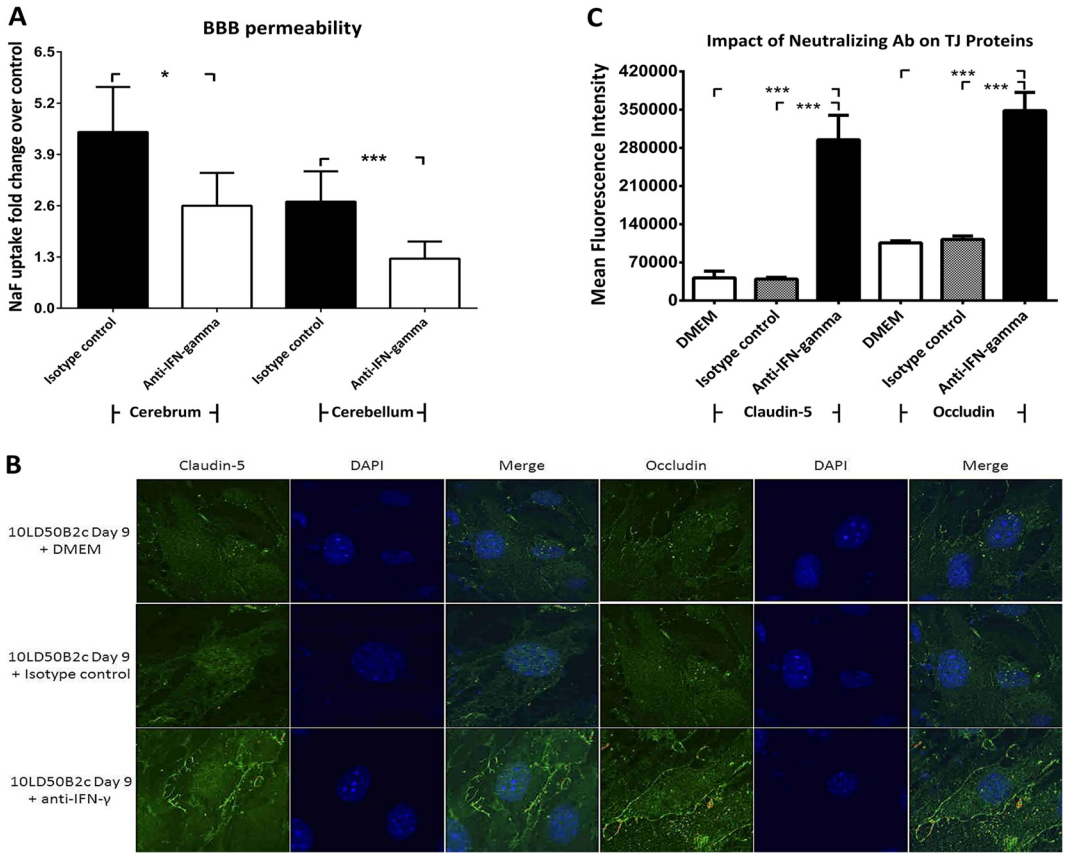

FIG 7 (A and B) IFN-γ neutralization ameliorates the enhancement of BBB permeability in RABV-infected mice (A) and the downregulation of TJ protein expression in BMECs treated with brain extracts from RABV-infected mice (B). (A) Female ICR mice infected i.c. with 10 LD_{50} of CVS-B2c were injected i.p. with 100 μg of an anti-IFN-γ neutralizing antibody or an isotype control antibody in PBS at 0, 2, and 4 days p.i. At day 6 p.i., BBB permeability was assessed by NaF uptake in the cerebrum and the cerebellum. Statistical analysis was performed with Student's *t* test. (B) Mouse BMECs were cocultured with brain extracts (treated either with DMEM, with 0.3 μg/ml of an anti-IFN-γ antibody, or with an isotype control antibody) from mice infected with 10 LD_{50} of CVS-B2c. After 24 h, BMECs were fixed and were stained either with DAPI and an anti-claudin-5 antibody or with DAPI and an anti-occludin antibody. The staining was visualized by confocal microscopy. (C) The MFIs at the ROI drawn around the cells under the different conditions were compared and analyzed statistically using one-way ANOVA followed by Tukey's *post hoc* test. Asterisks indicate statistical significance (*, $P < 0.05$; **, $P < 0.01$; ***, $P < 0.001$; ****, $P < 0.0001$).

virus (WNV) infection, it is neuronal CXCL10 that initiates the influx of $CD8^+$ T cells into the CNS. Neutralization of CXCL10 decreases the number of $CD8^+$ T cells in the brain and elevates mortality (51). It is not clear, however, whether it is resident neural cells or cells infiltrating from the periphery that produce CXCL10 and initiate the alteration of TJ proteins at the BBB after RABV infection.

In mice infected with wt RABV, TNF-α is located in the center of the molecular network. TNF-α has been shown to induce BBB disruption as a result of decreased transendothelial electrical resistance (TEER) of BMECs (53). Intraventricular injection of TNF-α into rats initiated an increased efflux of radiolabeled albumin into the cerebrospinal fluid (54). However, Saija et al. reported that intracarotid injection of TNF-α produced a significant decrease in BBB permeability to aminoisobutyric acid in rats (55). Others have shown that intracerebral injection of TNF-α does not alter BBB permeability in mice or rats (56, 57). The effects of TNF-α on BBB permeability in RABV infection are not clear (58, 59). CXCL10 was also upregulated in mice infected with DRV-Mexico; however, the expression level of CXCL10 was significantly lower than that in mice infected with CVS-B2c. Although CXCL10 can be stimulated by TNF-α (60), the expression level of CXCL10 remained low in mice infected with DRV-Mexico, possibly due to the lack of IFN-γ (60). In contrast, significantly high levels of CXCL10 were generated with the cooperation of IFN-γ and TNF-α, as shown in the network constructed for the CVS-B2c-infected group (Fig. 6A).

CXCL10, CXCL9, and CCL5 are three structurally and functionally related IFN-γ-inducible proteins; they bind to the receptor CXCR3 expressed on activated $CD4^+$ Th1 cells and function in governing the migration of lymphocytes into the CNS (61, 62). There is cross talk between IFN-γ, IL-12, and encephalitogenic $CD4^+$ Th1 signaling pathways (47). Thus, Th1 signaling pathways may play an important role in the enhancement of BBB permeability in mice infected with laboratory-attenuated RABV. Furthermore, analysis of canonical pathways in our study suggests that differential regulation of IL-17A production and IL-17A may be a key event in the BBB permeability enhancement observed in mice infected with laboratory-attenuated RABV. Therefore, we hypothesize that in the CNS, infection with RABV, particularly laboratory-attenuated RABV, stimulates the production of CXCL10 (other chemokines, such as CCL5 and CCL3, may also be in-

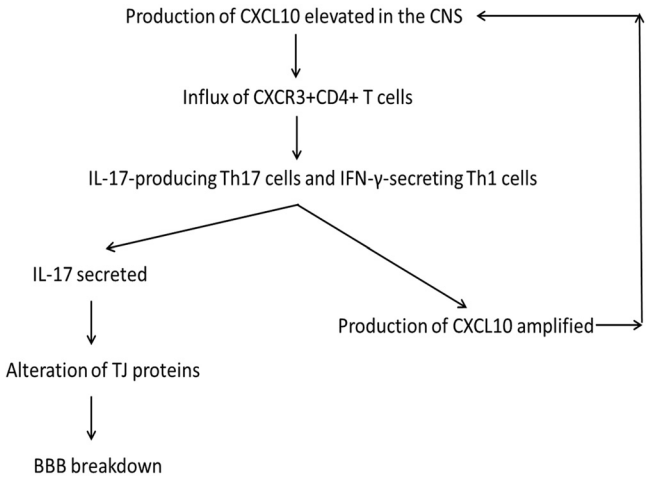

FIG 8 Schematic model for the mechanism(s) by which infection with laboratory-attenuated RABV induces the reduction of TJ protein expression and the enhancement of BBB permeability.

volved) in neural cells. These chemokines attract $CXCR3^+$ $CD4^+$ T cells infiltrating the CNS along the chemokine gradient and differentiating to IL-17-producing Th17 cells and IFN-γ-producing Th1 cells. This process has been shown to be the exclusive mechanism of leukocyte skewing in CNS inflammation (29). IL-17 produced by Th17 cells in the CNS initiates the alteration of TJ proteins in RABV infection. IFN-γ secreted by Th1 cells promotes the positive-feedback loop and amplifies CXCL10 production, $CXCR3^+$ CD4 T cell influx, and BBB breakdown (Fig. 8). The detection of significantly expressed IFN-γ at the later stage of infection further supports this hypothesis. Nevertheless, further studies are needed to demonstrate these pathways.

ACKNOWLEDGMENTS

We thank Abhijeet A. Bakre for helpful discussions regarding IPA data and James P. Barber for help in the Luminex assay.

This work was partially supported by Public Health Service grants AI-051560 and AI-093369 from the National Institute of Allergy and Infectious Diseases (to Z.F.F.).

We declare no conflict of interest.

REFERENCES

1. **Knobel DL, Cleaveland S, Coleman PG, Fevre EM, Meltzer MI, Miranda ME, Shaw A, Zinsstag J, Meslin FX.** 2005. Re-evaluating the burden of rabies in Africa and Asia. Bull. W. H. O. **83:**360–368.
2. **World Health Organization.** 2005. WHO Expert Consultation on Rabies: first report. WHO technical report series no. 931. World Health Organization, Geneva, Switzerland. http://www.who.int/rabies/ExpertConsultationOnRabies.pdf?ua=1.
3. **Rupprecht CE.** 1996. Rhabdoviruses: rabies virus, Chapter 61. *In* Baron S (ed), Medical microbiology, 4th ed. University of Texas Medical Branch at Galveston, Galveston, TX.
4. **Schnell MJ, McGettigan JP, Wirblich C, Papaneri A.** 2010. The cell biology of rabies virus: using stealth to reach the brain. Nat. Rev. Microbiol. **8:**51–61. http://dx.doi.org/10.1038/nrmicro2260.
5. **Suja MS, Mahadevan A, Madhusudana SN, Shankar SK.** 2011. Role of apoptosis in rabies viral encephalitis: a comparative study in mice, canine, and human brain with a review of literature. Patholog. Res. Int. **2011:** 374286. http://dx.doi.org/10.4061/2011/374286.
6. **Kuang Y, Lackay SN, Zhao L, Fu ZF.** 2009. Role of chemokines in the enhancement of BBB permeability and inflammatory infiltration after rabies virus infection. Virus Res. **144:**18–26. http://dx.doi.org/10.1016/j.virusres.2009.03.014.
7. **Zhao L, Toriumi H, Kuang Y, Chen H, Fu ZF.** 2009. The roles of chemokines in rabies virus infection: overexpression may not always be beneficial. J. Virol. **83:**11808–11818. http://dx.doi.org/10.1128/JVI.01346-09.
8. **Roy A, Phares TW, Koprowski H, Hooper DC.** 2007. Failure to open the blood-brain barrier and deliver immune effectors to central nervous system tissues leads to the lethal outcome of silver-haired bat rabies virus infection. J. Virol. **81:**1110–1118. http://dx.doi.org/10.1128/JVI.01964-06.
9. **Jackson AC, Randle E, Lawrance G, Rossiter JP.** 2008. Neuronal apoptosis does not play an important role in human rabies encephalitis. J. Neurovirol. **14:**368–375. http://dx.doi.org/10.1080/13550280802216502.
10. **Wang ZW, Sarmento L, Wang Y, Li XQ, Dhingra V, Tseggai T, Jiang B, Fu ZF.** 2005. Attenuated rabies virus activates, while pathogenic rabies virus evades, the host innate immune responses in the central nervous system. J. Virol. **79:**12554–12565. http://dx.doi.org/10.1128/JVI.79.19.12554-12565.2005.
11. **Sarmento L, Tseggai T, Dhingra V, Fu ZF.** 2006. Rabies virus-induced apoptosis involves caspase-dependent and caspase-independent pathways. Virus Res. **121:**144–151. http://dx.doi.org/10.1016/j.virusres.2006.05.002.
12. **Yan X, Prosniak M, Curtis MT, Weiss ML, Faber M, Dietzschold B, Fu ZF.** 2001. Silver-haired bat rabies virus variant does not induce apoptosis in the brain of experimentally infected mice. J. Neurovirol. **7:**518–527. http://dx.doi.org/10.1080/135502801753248105.
13. **Hooper DC, Scott GS, Zborek A, Mikheeva T, Kean RB, Koprowski H, Spitsin SV.** 2000. Uric acid, a peroxynitrite scavenger, inhibits CNS inflammation, blood-CNS barrier permeability changes, and tissue damage in a mouse model of multiple sclerosis. FASEB J. **14:**691–698.
14. **Hooper DC, Morimoto K, Bette M, Weihe E, Koprowski H, Dietzschold B.** 1998. Collaboration of antibody and inflammation in clearance of rabies virus from the central nervous system. J. Virol. **72:**3711–3719.
15. **Bennett J, Basivireddy J, Kollar A, Biron KE, Reickmann P, Jefferies WA, McQuaid S.** 2010. Blood-brain barrier disruption and enhanced vascular permeability in the multiple sclerosis model EAE. J. Neuroimmunol. **229:**180–191. http://dx.doi.org/10.1016/j.jneuroim.2010.08.011.
16. **Kean RB, Spitsin SV, Mikheeva T, Scott GS, Hooper DC.** 2000. The peroxynitrite scavenger uric acid prevents inflammatory cell invasion into the central nervous system in experimental allergic encephalomyelitis through maintenance of blood-central nervous system barrier integrity. J. Immunol. **165:**6511–6518.
17. **Faber M, Li J, Kean RB, Hooper DC, Alugupalli KR, Dietzschold B.** 2009. Effective preexposure and postexposure prophylaxis of rabies with a highly attenuated recombinant rabies virus. Proc. Natl. Acad. Sci. U. S. A. **106:**11300–11305. http://dx.doi.org/10.1073/pnas.0905640106.
18. **Wang H, Zhang G, Wen Y, Yang S, Xia X, Fu ZF.** 2011. Intracerebral administration of recombinant rabies virus expressing GM-CSF prevents the development of rabies after infection with street virus. PLoS One **6:**e25414. http://dx.doi.org/10.1371/journal.pone.0025414.
19. **Spindler KR, Hsu TH.** 2012. Viral disruption of the blood-brain barrier. Trends Microbiol. **20:**282–290. http://dx.doi.org/10.1016/j.tim.2012.03.009.
20. **Abbott NJ, Patabendige AA, Dolman DE, Yusof SR, Begley DJ.** 2010. Structure and function of the blood-brain barrier. Neurobiol. Dis. **37:**13–25. http://dx.doi.org/10.1016/j.nbd.2009.07.030.
21. **Lehner C, Gehwolf R, Tempfer H, Krizbai I, Hennig B, Bauer HC, Bauer H.** 2011. Oxidative stress and blood-brain barrier dysfunction under particular consideration of matrix metalloproteinases. Antioxid. Redox Signal. **15:**1305–1323. http://dx.doi.org/10.1089/ars.2011.3923.
22. **Rubin LL, Staddon JM.** 1999. The cell biology of the blood-brain barrier. Annu. Rev. Neurosci. **22:**11–28. http://dx.doi.org/10.1146/annurev.neuro.22.1.11.
23. **Pardridge WM.** 1999. Blood-brain barrier biology and methodology. J. Neurovirol. **5:**556–569. http://dx.doi.org/10.3109/13550289909021285.
24. **Toborek M, Lee YW, Flora G, Pu H, Andras IE, Wylegala E, Hennig B, Nath A.** 2005. Mechanisms of the blood-brain barrier disruption in HIV-1 infection. Cell. Mol. Neurobiol. **25:**181–199. http://dx.doi.org/10.1007/s10571-004-1383-x.
25. **Mathur A, Khanna N, Chaturvedi UC.** 1992. Breakdown of blood-brain barrier by virus-induced cytokine during Japanese encephalitis virus infection. Int. J. Exp. Pathol. **73:**603–611.
26. **Gralinski LE, Ashley SL, Dixon SD, Spindler KR.** 2009. Mouse adenovirus type 1-induced breakdown of the blood-brain barrier. J. Virol. **83:**9398–9410. http://dx.doi.org/10.1128/JVI.00954-09.
27. **Murphy AC, Lalor SJ, Lynch MA, Mills KH.** 2010. Infiltration of Th1 and Th17 cells and activation of microglia in the CNS during the course of

experimental autoimmune encephalomyelitis. Brain Behav. Immun. **24:** 641–651. http://dx.doi.org/10.1016/j.bbi.2010.01.014.
28. **Huppert J, Closhen D, Croxford A, White R, Kulig P, Pietrowski E, Bechmann I, Becher B, Luhmann HJ, Waisman A, Kuhlmann CR.** 2010. Cellular mechanisms of IL-17-induced blood-brain barrier disruption. FASEB J. **24:**1023–1034. http://dx.doi.org/10.1096/fj.09-141978.
29. **Shechter R, London A, Schwartz M.** 2013. Orchestrated leukocyte recruitment to immune-privileged sites: absolute barriers versus educational gates. Nat. Rev. Immunol. **13:**206–218. http://dx.doi.org/10.1038/nri3391.
30. **Zhang G, Fu ZF.** 2012. Complete genome sequence of a street rabies virus from Mexico. J. Virol. **86:**10892–10893. http://dx.doi.org/10.1128/JVI.01778-12.
31. **Morimoto K, Hooper DC, Carbaugh H, Fu ZF, Koprowski H, Dietzschold B.** 1998. Rabies virus quasispecies: implications for pathogenesis. Proc. Natl. Acad. Sci. U. S. A. **95:**3152–3156. http://dx.doi.org/10.1073/pnas.95.6.3152.
32. **Phares TW, Fabis MJ, Brimer CM, Kean RB, Hooper DC.** 2007. A peroxynitrite-dependent pathway is responsible for blood-brain barrier permeability changes during a central nervous system inflammatory response: TNF-α is neither necessary nor sufficient. J. Immunol. **178:**7334–7343.
33. **Trout JJ, Koenig H, Goldstone AD, Lu CY.** 1986. Blood-brain barrier breakdown by cold injury. Polyamine signals mediate acute stimulation of endocytosis, vesicular transport, and microvillus formation in rat cerebral capillaries. Lab. Invest. **55:**622–631.
34. **Li XQ, Sarmento L, Fu ZF.** 2005. Degeneration of neuronal processes after infection with pathogenic, but not attenuated, rabies viruses. J. Virol. **79:**10063–10068. http://dx.doi.org/10.1128/JVI.79.15.10063-10068.2005.
35. **Zhang G, Wang H, Mahmood F, Fu ZF.** 2013. Rabies virus glycoprotein is an important determinant for the induction of innate immune responses and the pathogenic mechanisms. Vet. Microbiol. **162:**601–613. http://dx.doi.org/10.1016/j.vetmic.2012.11.031.
36. **Wen Y, Wang H, Wu H, Yang F, Tripp RA, Hogan RJ, Fu ZF.** 2011. Rabies virus expressing dendritic cell-activating molecules enhances the innate and adaptive immune response to vaccination. J. Virol. **85:**1634–1644. http://dx.doi.org/10.1128/JVI.01552-10.
37. **Famakin B, Mou Y, Spatz M, Lawal M, Hallenbeck J.** 2012. Downstream Toll-like receptor signaling mediates adaptor-specific cytokine expression following focal cerebral ischemia. J. Neuroinflammation **9:**174. http://dx.doi.org/10.1186/1742-2094-9-174.
38. **Pfeiffer F, Schafer J, Lyck R, Makrides V, Brunner S, Schaeren-Wiemers N, Deutsch U, Engelhardt B.** 2011. Claudin-1 induced sealing of blood-brain barrier tight junctions ameliorates chronic experimental autoimmune encephalomyelitis. Acta Neuropathol. **122:**601–614. http://dx.doi.org/10.1007/s00401-011-0883-2.
39. **Argaw AT, Gurfein BT, Zhang Y, Zameer A, John GR.** 2009. VEGF-mediated disruption of endothelial CLN-5 promotes blood-brain barrier breakdown. Proc. Natl. Acad. Sci. U. S. A. **106:**1977–1982. http://dx.doi.org/10.1073/pnas.0808698106.
40. **Sporici R, Issekutz TB.** 2010. CXCR3 blockade inhibits T-cell migration into the CNS during EAE and prevents development of adoptively transferred, but not actively induced, disease. Eur. J. Immunol. **40:**2751–2761. http://dx.doi.org/10.1002/eji.200939975.
41. **Liao PH, Yang HH, Chou PT, Wang MH, Chu PC, Liu HL, Chen LK.** 2012. Sufficient virus-neutralizing antibody in the central nerve system improves the survival of rabid rats. J. Biomed. Sci. **19:**61. http://dx.doi.org/10.1186/1423-0127-19-61.
42. **Olofsson P, Johansson A, Wedekind D, Kloting I, Klinga-Levan K, Lu S, Holmdahl R.** 2004. Inconsistent susceptibility to autoimmunity in inbred LEW rats is due to genetic crossbreeding involving segregation of the arthritis-regulating gene Ncf1. Genomics **83:**765–771. http://dx.doi.org/10.1016/j.ygeno.2003.10.005.
43. **Dallasta LM, Pisarov LA, Esplen JE, Werley JV, Moses AV, Nelson JA, Achim CL.** 1999. Blood-brain barrier tight junction disruption in human immunodeficiency virus-1 encephalitis. Am. J. Pathol. **155:**1915–1927. http://dx.doi.org/10.1016/S0002-9440(10)65511-3.
44. **Toneatto S, Finco O, van der Putten H, Abrignani S, Annunziata P.** 1999. Evidence of blood-brain barrier alteration and activation in HIV-1 gp120 transgenic mice. AIDS **13:**2343–2348. http://dx.doi.org/10.1097/00002030-199912030-00005.
45. **Eugenin EA, Osiecki K, Lopez L, Goldstein H, Calderon TM, Berman JW.** 2006. CCL2/monocyte chemoattractant protein-1 mediates enhanced transmigration of human immunodeficiency virus (HIV)-infected leukocytes across the blood-brain barrier: a potential mechanism of HIV-CNS invasion and NeuroAIDS. J. Neurosci. **26:**1098–1106. http://dx.doi.org/10.1523/JNEUROSCI.3863-05.2006.
46. **Boven LA, Middel J, Verhoef J, De Groot CJ, Nottet HS.** 2000. Monocyte infiltration is highly associated with loss of the tight junction protein zonula occludens in HIV-1-associated dementia. Neuropathol. Appl. Neurobiol. **26:**356–360. http://dx.doi.org/10.1046/j.1365-2990.2000.00255.x.
47. **Lovett-Racke AE, Yang Y, Racke MK.** 2011. Th1 versus Th17: are T cell cytokines relevant in multiple sclerosis? Biochim. Biophys. Acta **1812:**246–251. http://dx.doi.org/10.1016/j.bbadis.2010.05.012.
48. **Stromnes IM, Cerretti LM, Liggitt D, Harris RA, Goverman JM.** 2008. Differential regulation of central nervous system autoimmunity by T_H1 and T_H17 cells. Nat. Med. **14:**337–342. http://dx.doi.org/10.1038/nm1715.
49. **Stamatovic SM, Keep RF, Kunkel SL, Andjelkovic AV.** 2003. Potential role of MCP-1 in endothelial cell tight junction 'opening': signaling via Rho and Rho kinase. J. Cell Sci. **116:**4615–4628. http://dx.doi.org/10.1242/jcs.00755.
50. **Tanuma N, Sakuma H, Sasaki A, Matsumoto Y.** 2006. Chemokine expression by astrocytes plays a role in microglia/macrophage activation and subsequent neurodegeneration in secondary progressive multiple sclerosis. Acta Neuropathol. **112:**195–204. http://dx.doi.org/10.1007/s00401-006-0083-7.
51. **Klein RS, Lin E, Zhang B, Luster AD, Tollett J, Samuel MA, Engle M, Diamond MS.** 2005. Neuronal CXCL10 directs $CD8^+$ T-cell recruitment and control of West Nile virus encephalitis. J. Virol. **79:**11457–11466. http://dx.doi.org/10.1128/JVI.79.17.11457-11466.2005.
52. **Devaraj S, Jialal I.** 2009. Increased secretion of IP-10 from monocytes under hyperglycemia is via the TLR2 and TLR4 pathway. Cytokine **47:**6–10. http://dx.doi.org/10.1016/j.cyto.2009.02.004.
53. **de Vries HE, Blom-Roosemalen MC, van Oosten M, de Boer AG, van Berkel TJ, Breimer DD, Kuiper J.** 1996. The influence of cytokines on the integrity of the blood-brain barrier in vitro. J. Neuroimmunol. **64:**37–43. http://dx.doi.org/10.1016/0165-5728(95)00148-4.
54. **Dickstein JB, Moldofsky H, Hay JB.** 2000. Brain-blood permeability: TNF-α promotes escape of protein tracer from CSF to blood. Am. J. Physiol. Regul. Integr. Comp. Physiol. **279:**R148–R151.
55. **Saija A, Princi P, Lanza M, Scalese M, Aramnejad E, De Sarro A.** 1995. Systemic cytokine administration can affect blood-brain barrier permeability in the rat. Life Sci. **56:**775–784. http://dx.doi.org/10.1016/0024-3205(95)00008-T.
56. **Petito CK, Adkins B, Tracey K, Roberts B, Torres-Munoz J, McCarthy M, Czeisler C.** 1999. Chronic systemic administration of tumor necrosis factor alpha and HIV gp120: effects on adult rodent brain and blood-brain barrier. J. Neurovirol. **5:**314–318. http://dx.doi.org/10.3109/13550289909015818.
57. **Schnell L, Fearn S, Schwab ME, Perry VH, Anthony DC.** 1999. Cytokine-induced acute inflammation in the brain and spinal cord. J. Neuropathol. Exp. Neurol. **58:**245–254. http://dx.doi.org/10.1097/00005072-199903000-00004.
58. **Mark KS, Miller DW.** 1999. Increased permeability of primary cultured brain microvessel endothelial cell monolayers following TNF-α exposure. Life Sci. **64:**1941–1953. http://dx.doi.org/10.1016/S0024-3205(99)00139-3.
59. **Liu H, Luiten PG, Eisel UL, Dejongste MJ, Schoemaker RG.** 2013. Depression after myocardial infarction: TNF-α-induced alterations of the blood-brain barrier and its putative therapeutic implications. Neurosci. Biobehav. Rev. **37:**561–572. http://dx.doi.org/10.1016/j.neubiorev.2013.02.004.
60. **Ohmori Y, Hamilton TA.** 1995. The interferon-stimulated response element and a κB site mediate synergistic induction of murine IP-10 gene transcription by IFN-γ and TNF-α. J. Immunol. **154:**5235–5244.
61. **Müller M, Carter S, Hofer MJ, Campbell IL.** 2010. The chemokine receptor CXCR3 and its ligands CXCL9, CXCL10 and CXCL11 in neuroimmunity—a tale of conflict and conundrum. Neuropathol. Appl. Neurobiol. **36:**368–387. http://dx.doi.org/10.1111/j.1365-2990.2010.01089.x.
62. **Liu L, Huang D, Matsui M, He TT, Hu T, Demartino J, Lu B, Gerard C, Ransohoff RM.** 2006. Severe disease, unaltered leukocyte migration, and reduced IFN-γ production in $CXCR3^{-/-}$ mice with experimental autoimmune encephalomyelitis. J. Immunol. **176:**4399–4409.